Int. J. Electrochem. Sci., 14 **(2019)** 494 – 505, doi: 10.20964/2019.01.27

International Journal of
ELECTROCHEMICAL
SCIENCE
www.electrochemsci.org

Thermal Stability of $[Ni(htde)](ClO_4)_2$ and Its Corrosion Inhibition Effect for Mild Steel in 1.0 M HCl and H_2SO_4 Solutions

Wan Gou[1], *Bin Xie*[2,*], *Chong Xu*[2,3], *Zhi Zheng*[2,3], *Jiajun He*[2,3], *Dan Huang*[2,3], *Na Geng*[2,3]

[1] Eastern Sichuan Sub-center of National Engineering Research Center for Municipal Wastewater Treatment and Reuse, Sichuan University of Arts and Science, Dazhou 635000, China
[2] School of Materials Science and Engineering, Sichuan University of Science and Engineering, Zigong 643000, China
[3] School of Chemistry and Chemical Engineering, Sichuan University of Arts and Science, Dazhou 635000, China
[*]E-mail: xiebinsuse@163.com

Received: 5 August 2018 / *Accepted:* 16 September 2018 / *Published:* 30 November 2018

In this study, the nickel (II) complex of 5, 7, 7, 12, 14, 14-hexamethyl-1, 4, 8, 11-tetraazacyclotetradeca4, 11-diene ($[Ni(htde)](ClO_4)_2$) is synthesized and the thermal stability of $[Ni(htde)](ClO_4)_2$ also studied by TG/DSC technology, while its corrosion inhibition for mild steel (MS) in 1.0 M HCl and H_2SO_4 solutions is studied by potentiodynamic polarization and weight loss measurements. Results findings that the thermal decomposition process of $[Ni(htde)](ClO_4)_2$ in N_2 and air atmospheres all proceeded in three steps, and the thermal decomposition is not affected by N_2 and air atmospheres, which can be stable at the temperature below 270 °C under these two atmospheres. $[Ni(htde)](ClO_4)_2$ is a mixed-type inhibitor, the inhibition efficiency increases with the increase of $[Ni(htde)](ClO_4)_2$ concentration. And the adsorption of $[Ni(htde)](ClO_4)_2$ on MS surface can be described by Langmuir isotherm, which belongs to physic- and chemisorption.

Keywords: Macrocycle; Thermal stability; Decomposition; Corrosion inhibition; Acid.

1. INTRODUCTION

Metal material is one of the most important engineering materials, and its corrosion problem is always an important problem when it is widely used in various fields. Among many metal materials, the different types of steel have been outstanding in application due to its unique advantages. However, while it is widely used, the corrosion problem also brings many limitations. This is not only because corrosion can cause damage, environmental pollution and resource waste, but more importantly, it can

cause major safety hazards. Therefore, corrosion of metal materials is not only an economic problem, but also a social problem [1-2]. Various methods are used to decrease the corrosion of metals exposing in acids solution, weather, or other hostile environments [3-5]. As everyone knows, that using corrosion inhibitor is one of the most effective, common and economical method for corrosion protecting. Among the various corrosion inhibitors, organic inhibitors can be used as a kind of corrosion inhibitors with excellent performance [6-8]. Generally, most of corrosion inhibitors contain heteroatoms in their molecular structure, such as nitrogen atoms, sulfur atoms, oxygen atoms and so on [9-11]. These heteroatoms will cause the inhibitor molecules to adsorb on metal surface, thus preventing the corrosion medium from attacking the metal to achieve the purpose of inhibiting corrosion [7-11].

Macrocycles are often described as a molecule containing at least one large ring composed of 12 or more atoms [12]. In the past, most of the known synthetic macrocycles had been prepared, characterized and reported in references [13-17]. Most commonly they are quadridentates containing nitrogen donor atoms, although compounds containing sulfur and oxygen donor atoms and are also known [13-17]. These macrocycles compounds containing heteroatoms (N, S, P and O) are likely to be the potential corrosion inhibitors to prevent or decrease the corrosion rate of metals in different corrosion environments.

As the classical macrocycles, the unsaturated macrocycle of 5, 7, 7, 12, 14, 14-hexamethyl-1, 4, 8, 11-tetraazacyclotetradeca-4, 11-diene diperchlorate and saturated macrocycle of 5, 5, 7, 12, 12, 14-hexamethyl-1, 4, 8, 11-tetraazacyclotetradecane as corrosion inhibitor were reported in our previous works [18-19]. Here, the nickel (II) complex of 5, 7, 7, 12, 14, 14-hexamethyl-1, 4, 8, 11-tetraazacyclotetradeca 4, 11-diene ($[Ni(htde)](ClO_4)_2$) is synthesized, and as a further extension study, this work will explore the thermal stability of $[Ni(htde)](ClO_4)_2$ and its corrosion inhibition for mild steel in 1.0 M HCl and H_2SO_4 solutions.

2. MATERIALS AND METHODS

2.1 Materials

The chemicals (A. R.) of methanol, acetone, ethylenediamine, nickel (II) acetate tetrahydrate, diethyl ether, hydrochloric acid (37%) and sulfuric acid (98%) were purchased from Kelong Chemical Reagent Co. Ltd. (Chengdu). Meanwhile, the perchloric acid (72%) is purchased from Tianjin xinyuan chemical Co. Ltd (Tianjin). The test samples with the sizes of 2×25×50 mm (S = 28.0 cm^2) and the working electrode encapsulated by teflon with the working area of 0.785 cm^2 all prepared by mild steel (MS).

2.2 Synthesis of $[Ni(htde)](ClO_4)_2$

Dissolve 50 g nickel (II) acetate tetrahydrate ($Ni(CH_3COO)_2{\cdot}4H_2O$, 0.2 mol) in 500 ml methanol in a 1 L beaker, then 90 g 5, 7, 7, 12, 14, 14- hexamethyl-1, 4, 8, 11-tetraazacyclotetradeca 4, 11-diene diperchlorate (0.19 mol) as macrocyclic ligand is added, and see the reference [20] for synthesis. A slight

excess of nickel (II) acetate tetrahydrate is needed to ensure the complete reaction for the macrocyclic ligand. When nickel (II) acetate tetrahydrate and the macrocyclic ligand are fully mixed in methanol, which would be stirred for 5 hours at 50 °C and cooled rapidly in a refrigerator, and the yellow crystals of the racemic isomer are removed by filtration. The crystals are washed with methanol and diethyl ether and dried in a vacuum oven at 60 °C for 4 hours. Here, the target nickel (II) complex of $[Ni(htde)](ClO_4)_2$ is shown in figure 1.

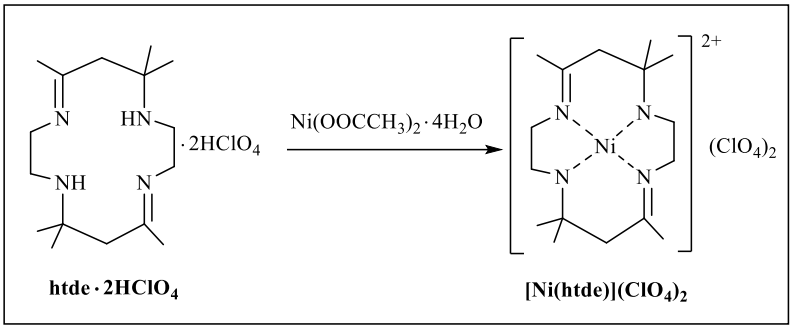

Figure 1. Reaction and structure of the target nickel (II) complex of $[Ni(htde)](ClO_4)_2$.

2.3 Thermal stability of $[Ni(htde)](ClO_4)_2$

The thermal stability evaluation by thermogravimetric analysis (TG) and differential scanning calorimetry (DSC) analyses were performed with the Netzsch STA 409 PC/PG thermal analyzer (Germany) in temperature range from 25 °C to 850 °C at the heating rates of 5 °C min^{-1}, 10 °C min^{-1} and 20 °C min^{-1}. The measurement on thermal analysis were taken using sample masses of 6.0-8.0 mg in open alumina sample holders under both dynamic dry air and N_2 atmospheres with a discharge rate of 100 mL min^{-1} at atmosphere pressure.

2.4 Corrosion inhibition evaluation of $[Ni(htde)](ClO_4)_2$

Weight loss measurement (method I): This method was described in different works [21-22]. Here, the corrosion rate (v) and inhibition efficiency (IE_{WL}, %) of MS corrosion in 1.0 M HCl and H_2SO_4 medium with and without different concentrations of $[Ni(htde)](ClO_4)_2$ were calculated by equation (1) and (2). Where m_0 and m_i are the mass of the test specimen before and after corrosion, S = 28.0 cm^2, t is the immersion time, v_i and v_0 are corrosion rate of the MS specimen in acid solutions with and without different concentrations $[Ni(htde)](ClO_4)_2$.

$$v_i = \frac{m_0 - m_i}{St} \quad (1)$$

$$IE_{WL}\,(\%) = \frac{v_0 - v_i}{v_0} \times 100\% \quad (2)$$

Potentiodynamic polarization measurement (method II): The method was employed by CHI 660D electrochemical workstation choosing the Pt electrode and SCE (saturated calomel reference electrode) as the counter and reference electrode, the potential sweep rate was 0.5 mV s^{-1}. The inhibition efficiency (IE_{Tafel}, %) can be calculated by equation (3) [23-24]. In this equation, I_i and I_0 are the

corrosion current density values of MS corrosion in acid solutions with and without different concentrations [Ni(htde)]$(ClO_4)_2$.

$$IE_{\text{Tafel}}\ (\%) = \frac{I_0 - I_i}{I_0} \times 100\% \qquad (3)$$

3. RESULTS AND DISCUSSION

3.1 Thermal stability of [Ni(htde)]$(ClO_4)_2$

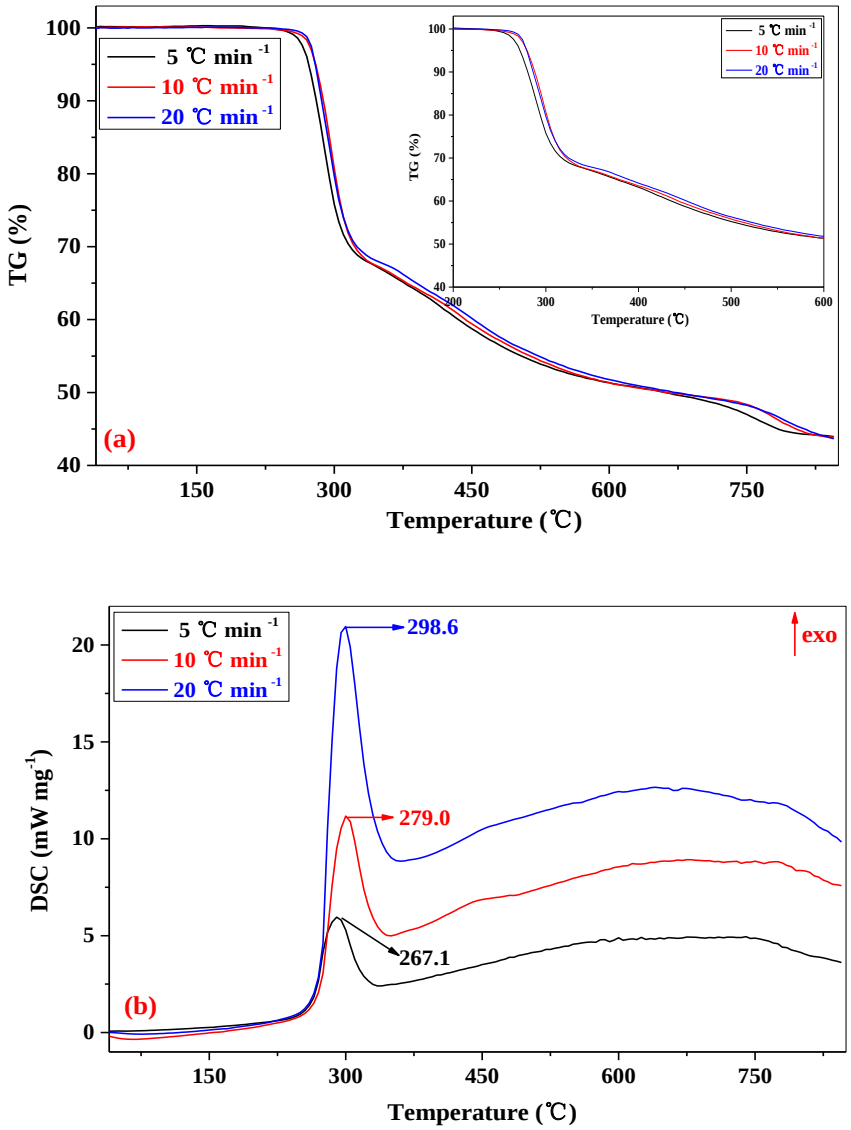

Figure 2. TG curves (a) and DSC curves (b) of [Ni(htde)]$(ClO_4)_2$ in N_2 atmosphere at the heating rates of 5, 10 and 20 °C min^{-1}.

The thermal stability and decomposition of [Ni(htde)]$(ClO_4)_2$ was studied by TG/DSC. Here, the TG curves and DSC curves obtained under the N_2 atmosphere at the heating rates of 5, 10 and 20 °C min^{-1} are presented in figure 2 (a) and (b).

From the TG curves showing in figure 2 (a), which reveal that the thermal decomposition process of $[Ni(htde)](ClO_4)_2$ in N_2 atmosphere at 5, 10 and 20 °C min^{-1} all proceeded in three steps. The first step attribute to the thermal oxidation degradation of macrocyclic ligand (htde) by perchlorate (ClO_4^-) in the temperature range from 270 °C to 310 °C. The second step in the temperature range of 310 - 540 °C is corresponding to the decomposition of oxidation products obtained by the first step. And the third step of mass loss in the temperature range of 540-800 °C, it is caused by the complex reactions of decomposition products at high temperatures (＞ 540 °C). Under TG analysis conditions, although the heating rate is different, all the TG curves changes very slightly. Moreover, it can be found that $[Ni(htde)](ClO_4)_2$ demonstrates mass loss 29.63%, 17.25% and 8.95% in the first, second and third step at the heating rate of 5 °C min^{-1}, respectively.

At the same time, the TG curves show that the mass loss of the compound of $[Ni(htde)](ClO_4)_2$ do not destruct at the temperature below 270 °C, which further suggests that the compound of $[Ni(htde)](ClO_4)_2$ can be stable at the temperature below 270 °C under the N_2 atmosphere.

Based on the DSC curves presenting in figure 2 (b), it can't find any obvious endothermic peaks during heating of $[Ni(htde)](ClO_4)_2$ in N_2 atmosphere at different heating rates, but instead there are three strong exothermic peaks at 267.1 °C, 279.0°C and 298.6 °C with the heating rates of 5, 10 and 20 °C min^{-1}.

So it is conferred that the process of heating $[Ni(htde)](ClO_4)_2$ is a self-oxidation and destruction process between perchlorate (ClO_4^-) and macrocyclic ligand (htde), which belongs to a strong exothermic process. In the heating process, the heat released will cover up with the heat absorbed, so only exothermic peaks will present in the curves instead of endothermic peaks.

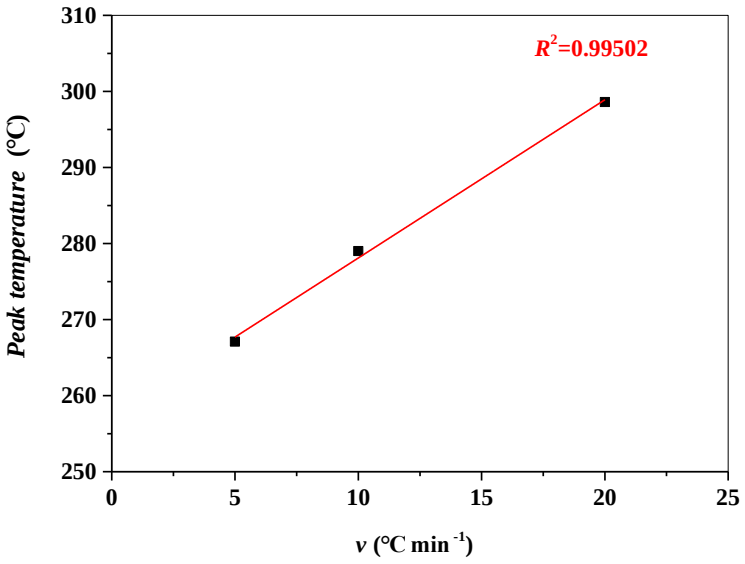

Figure 3. Fitting result between exothermic peak temperature and heating rates for $[Ni(htde)](ClO_4)_2$ heating in N_2 atmosphere.

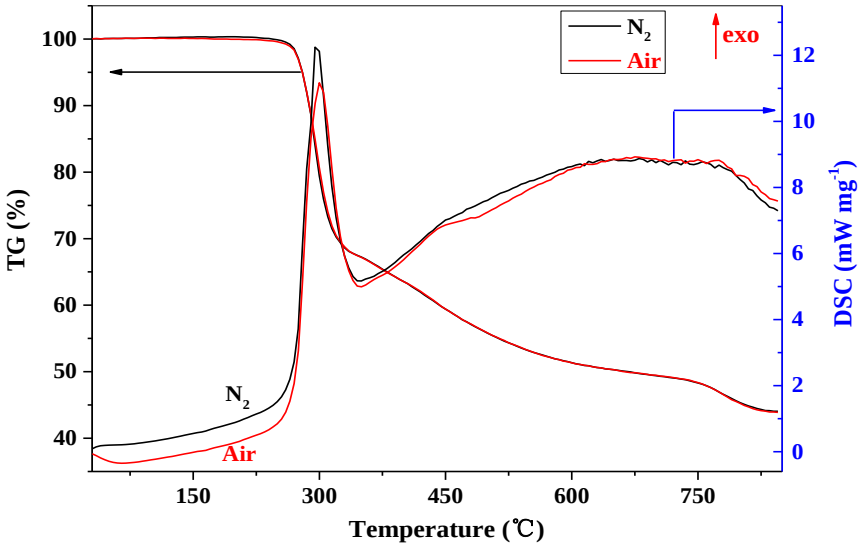

Figure 4. TG/DSC curves for heating [Ni(htde)]$(ClO_4)_2$ in air and N_2 atmospheres at 10 °C min^{-1}.

In addition, the fitting result between the temperature of exothermic peaks and heating rates for [Ni(htde)]$(ClO_4)_2$ heating in N_2 atmosphere is shown in figure 3. It can be seen from the figure that the temperature of exothermic peaks (T_P, °C) increases with the increase of the heating rates (v, °C min^{-1}), and there is a strong linear relationship (R^2 = 0.99502) between the heating rates and the peaks temperature, which can be expressed by T_P (°C) = 257.3 + 2.08 v.

Moreover， the thermal stability of [Ni(htde)]$(ClO_4)_2$ in different atmospheres (air and N_2) is studied by TG/DSC curves for heating [Ni(htde)]$(ClO_4)_2$ at 10 °C min^{-1} presenting in figure 4. Comparison TG curves and DSC curves obtained under the N_2 and air atmospheres, it is not difficult to find that the TG curve is almost the same variation tendency in the figure with [Ni(htde)]$(ClO_4)_2$ heated in N_2 and air atmospheres. This indicates that the thermal decomposition mechanism for [Ni(htde)]$(ClO_4)_2$ heating is not affected by N_2 and air atmospheres. Under the temperature below 270 °C, the DSC curve does not overlap, which may be due to the baseline drift during the test.

3.2 Potentiodynamic polarization measurement

Figure 5 (a) and (b) reveal the polarization curves of MS corrosion in 1.0 M HCl and 1.0 M H_2SO_4 with various concentrations of [Ni(htde)]$(ClO_4)_2$ at 30 °C obtained by potentiodynamic polarization measurement. Meanwhile, the E (V), I (μA cm^{-2}), β_c (mV dec^{-1}), β_a (mV dec^{-1}) and IE_{Tafel} (%) are listed in table 1.

From figure 5 (a), (b) and table 1, both anodic and cathodic curves shift to lower current densities in 1.0 M HCl and 1.0 M H_2SO_4 with various concentrations of [Ni(htde)]$(ClO_4)_2$. This indicates that [Ni(htde)]$(ClO_4)_2$ can decrease the corrosion rate of MS in 1.0 M HCl and 1.0 M H_2SO_4. The corrosion current densities increase with the concentration of [Ni(htde)]$(ClO_4)_2$, indicating with the increase of inhibitor concentration that the corrosion inhibition effect gradually improved. This is due to the higher concentration of [Ni(htde)]$(ClO_4)_2$ is more conducive to form the protective film on surface, thus

hindering the corrosion of MS in HCl and H_2SO_4 by hydrogen ions. When the corrosion inhibitor concentration is 200 mg L^{-1}, the inhibition efficiency (IE_{Tafel},%) for MS corrosion 1.0 M HCl and 1.0 M H_2SO_4 are 64.63% and 81.23%, respectively. Additionally, the all the shifts of *E* (corrosion potential, V) less than 80 mV (< 35 mV) show that [Ni(htde)]$(ClO_4)_2$ is a mixed-type inhibitor [18, 23 24]. Comparing [Ni(htde)]$(ClO_4)_2$ with reported macrocyclic inhibitors of 5, 7, 7, 12, 14, 14-hexame- thyl-1, 4, 8, 11-tetraazacyclotetradeca-4, 11-diene diperchlorate (unsaturated macrocycle) and 5, 5, 7, 12, 12, 14- hexamethyl-1, 4, 8, 11-tetraazacyclotetradecane (saturated macrocycle) [18, 19], it can be found the corrosion inhibition of [Ni(htde)]$(ClO_4)_2$ is not as good as unsaturated macrocycle (92.86%) and saturated macrocycle (93.79%) adding in HCl solution.

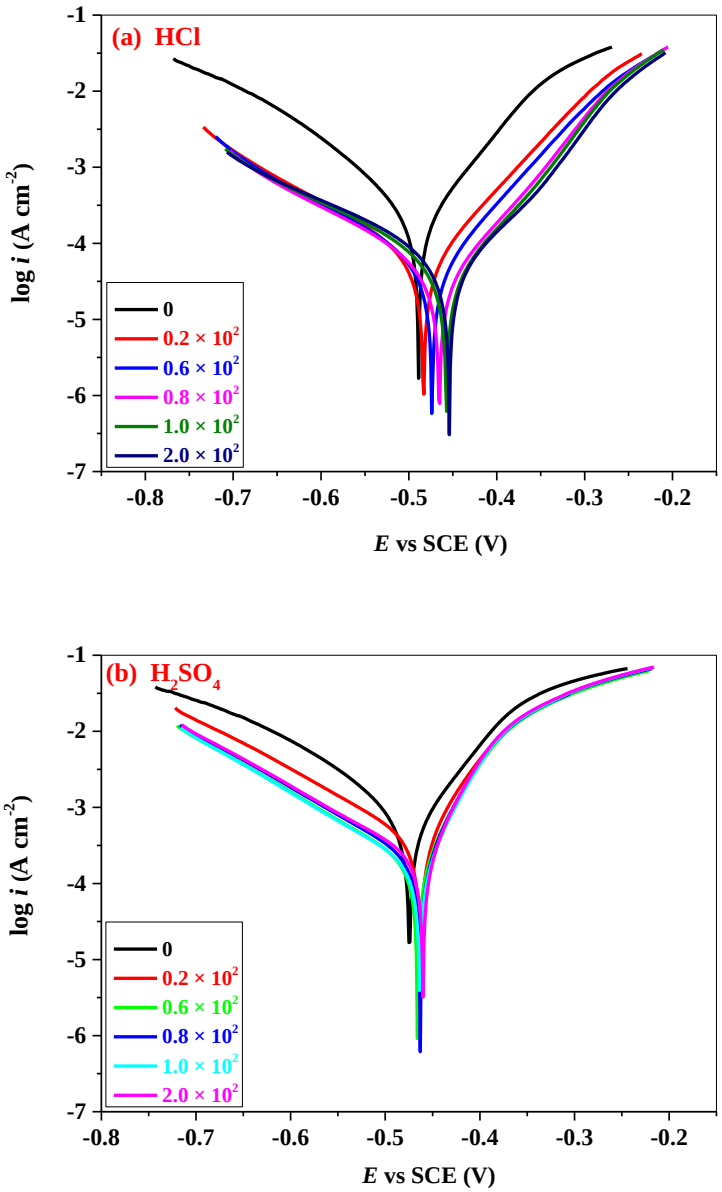

Figure 5. The polarization curves for MS in 1.0 M HCl (a) and 1.0 M H_2SO_4 (b) with various concentrations of [Ni(htde)]$(ClO_4)_2$.

Table 1. Polarization parameters for MS in 1.0 M HCl and 1.0 M H_2SO_4 with various concentrations of [Ni(htde)]$(ClO_4)_2$.

Corrosion Solution	*C* (mg L^{-1})	*E* (V)	*I* (μA cm^{-2})	β_c (mV dec^{-1})	β_a (mV dec^{-1})	IE_{Tafel} (%)
HCl	0	- 0.489	695.58	106.71	70.23	-
	20	- 0.483	209.66	150.60	79.91	69.86
	60	- 0.474	168.53	155.38	77.78	75.77
	80	- 0.465	170.02	170.30	80.98	75.56
	100	- 0.457	146.73	159.18	75.41	78.91
	200	- 0.454	130.58	151.52	76.22	81.23
H_2SO_4	0	- 0.475	2440.0	125.41	74.77	-
	20	- 0.463	1822.3	141.24	88.56	25.32
	60	- 0.466	1136.3	136.97	78.09	53.43
	80	- 0.463	962.8	138.89	83.72	60.54
	100	- 0.464	923.9	137.95	79.59	62.14
	200	- 0.460	863.0	143.68	80.67	64.63

3.3 Weight loss measurement

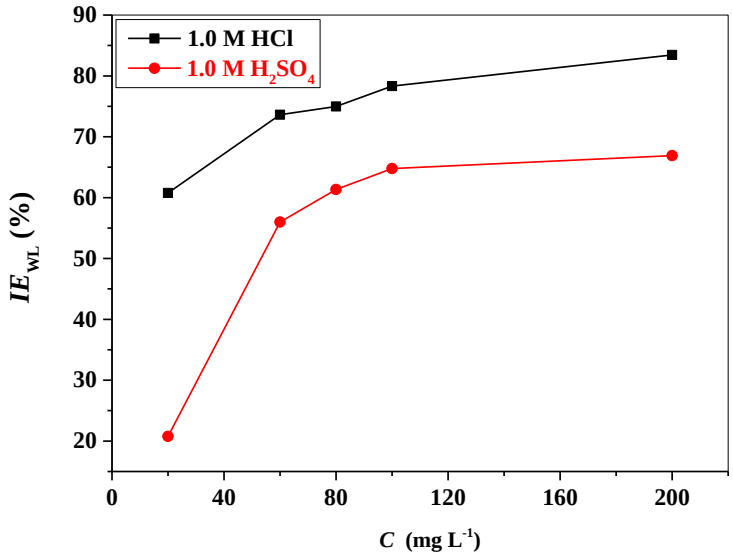

Figure 6. Relationships between the concentration of [Ni(htde)]$(ClO_4)_2$ and inhibition efficiency.

Figure 6 demonstrate the relationships between the concentration of [Ni(htde)]$(ClO_4)_2$ (*C*, mg L^{-1}) and inhibition efficiency (IE_{WL},%) for the inhibitor added in 1.0 M HCl and H_2SO_4 solutions for MS corrosion at 30 °C. It can be seen from this figure that the inhibition efficiency increases with the increase of the concentration of [Ni(htde)]$(ClO_4)_2$ in both 1.0 M HCl and H_2SO_4 solutions. When the concentration of corrosion inhibitor is higher than 100 mg L^{-1}, the inhibition efficiency tends to be stable with the change of [Ni(htde)]$(ClO_4)_2$ concentration. This is caused by the balance of the adsorption and desorption of inhibitor molecules on MS surface. By comparing the corrosion inhibition performance of

$[Ni(htde)](ClO_4)_2$ in 1.0 M HCl and H_2SO_4 solutions, it is easy to know that the inhibitory effect of $[Ni(htde)](ClO_4)_2$ in HCl for MS corrosion is better than that in H_2SO_4 solution. This also indicates that the $[Ni(htde)](ClO_4)_2$ is more suitable for using in HCl solution. When the concentration of $[Ni(htde)](ClO_4)_2$ is 100 mg L^{-1}, the inhibition efficiencies are 78.33% and 64.77%, respectively.

According to the molecular structure of $[Ni(htde)](ClO_4)_2$ showing in figure 1, it is speculated that the corrosion inhibition performance of $[Ni(htde)](ClO_4)_2$ is probably affected by two factors. On the one hand, the perchlorate (ClO_4^-) in $[Ni(htde)](ClO_4)_2$ molecular structure has the oxidation property, which can lead to the formation of oxide film on the MS surface and thus play a role in corrosion inhibition. On the other hand, due to the macrocyclic ligand (htde) obtained from $[Ni(htde)](ClO_4)_2$ dissociation under acidic conditions, resulting the lone pair electrons of N atoms presenting in htde can interact with iron atoms on the surface of MS thus showing the corrosion inhibition. Therefore, the corrosion inhibition of $[Ni(htde)](ClO_4)_2$ is caused by both the oxidation of perchlorate and the adsorption of N atoms.

3.4 Adsorption isotherm

According to the data presenting in figure 6, various isotherms [18, 25-26] are employed to study the adsorption of $[Ni(htde)](ClO_4)_2$ on MS surface in 1.0 M HCl and H_2SO_4 solutions. Meanwhile, the Langmuir adsorption isotherm ($C/\theta = 1/K + C$, $\theta = (v_0 - v_i)/v_0$) [25, 26, 27-28] fitting results are presented in figure 7 (a) and (b). Where C is$[Ni(htde)](ClO_4)_2$ concentration, K is the adsorption equilibrium constant and θ is the surface coverage, v_i and v_0 are the corrosion rate of MS corrosion in acid solutions with and without different concentrations of inhibitor. In the two figures, C/θ versus C show the strong linear relationship for MS corrosion in 1.0 M HCl and H_2SO_4 solutions with the concentration of $[Ni(htde)](ClO_4)_2$ from 20 mg L^{-1} to 200 mg L^{-1} (R^2 = 0.99907) and 60 mg L^{-1} to 200 mg L^{-1} (R^2 = 0.99754) at 30 °C, which suggest that the adsorption of $[Ni(htde)](ClO_4)_2$ on MS surface can be described by Langmuir isotherm. The adsorption standard free energy (ΔG) can be obtained by equation of $\Delta G = -RT\ln(55.5K)$, which are -36.97 kJ mol^{-1} (1.0 M HCl) and -35.79 kJ mol^{-1} (1.0 M H_2SO_4).

The ΔG both higher than -40.00 kJ mol^{-1} show that the adsorption processes of $[Ni(htde)](ClO_4)_2$ on MS surface in HCl and H_2SO_4 solutions all belongs to the mixed adsorption which involve both the physic- and chemisorption [18, 19]. However, it is not difficult to find that when the concentration of $[Ni(htde)](ClO_4)_2$ is lower than 60 mg L^{-1} for MS in 1.0 M H_2SO_4 solution that the adsorption of the inhibitor on MS surface does not conform to the Langmuir adsorption isotherm (R^2 = 0.93900).

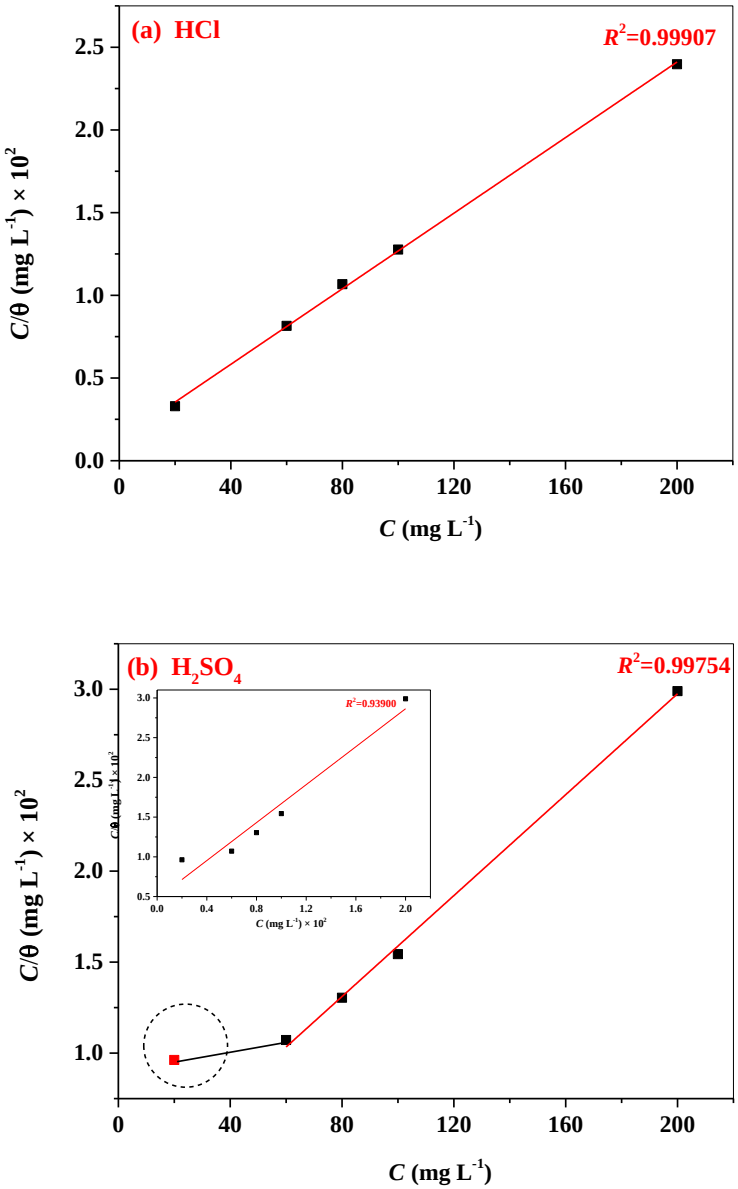

Figure 7. The plots of Langmuir adsorption isotherm for [Ni(htde)]$(ClO_4)_2$ on MS in 1.0 M HCl (a) and 1.0 M H_2SO_4 (b).

4. CONCLUSIONS

In this work, the nickel (II) complex of 5, 7, 7, 12, 14, 14-hexamethyl-1, 4, 8, 11-tetraaza-cyclotetradeca4, 11-diene ([Ni(htde)]$(ClO_4)_2$) was successfully synthesized. The study results show that the thermal decomposition process of [Ni(htde)]$(ClO_4)_2$ in N_2 and air atmospheres all proceeded in three steps, and the thermal decomposition is not affected by N_2 and air atmospheres, which can be stable at temperature below 270 °C. [Ni(htde)]$(ClO_4)_2$ as the new corrosion inhibitor is a mixed-type inhibitor, the inhibition efficiency increases with the increase of [Ni(htde)]$(ClO_4)_2$ concentration. Moreover, the

adsorption of [Ni(htde)]$(ClO_4)_2$ on mild steel surface can be described by Langmuir isotherm, which belongs to physic- and chemisorption.

ACKNOWLEDGMENTS

This project is supported by the Program of Education Department of Sichuan Province (Nos. 17ZB0371, 18CZ0038), the program of Science and Technology Department of Sichuan Province (No. 2018JY0061), the opening project of Material Corrosion and Protection Key Laboratory of Sichuan Province (No. 2017CL02), the Key Laboratories of Fine Chemicals and Surfactants in Sichuan Provincial Universities (Nos. 2018JXZ01, 2016JXZ03), the Key Laboratories of Green Catalysis of Higher Education Institutes of Sichuan (No. LZJ1803).

References

1. P. A. Lozada, O. O. Xometl, N. V. Likhanova, I. V .Lijanova, J. R.Vargas-García and R. E. H. Ramírez*, J. Mol. Liq*., 265 (2018) 151.
2. H. J. Habeeb, H. M. Luaibi, R. M. Dakhil, A. A. H. Kadhum, A. A. Al-Amiery and T. S. Gaaz, *Res. Phys.,* 8 (2018) 1260.
3. Y. Xue, X. Pang, B. Jiang and H. Jahed*, Int. J. Electrochem. Sci.,* 13 (2018) 7265.
4. L. Wang, J. Wang and W. Hu, *Int. J. Electrochem. Sci*., 13 (2018) 7356.
5. L. M. Quej-Aké, A. Contreras and J. Aburto, *Int. J. Electrochem. Sci*., 13 (2018) 7416.
6. A. E.Vazquez, F. J. R. Gomez1, E. Juaristi, M. E. Casao, G. E. N. Silva, D. A. Beltrán and M. P. Pardave, *Int. J. Electrochem. Sci*., 13 (2018) 7517.
7. H. Yang, M. Zhang and A. Singh, *Int. J. Electrochem. Sci*., 13 (2018) 9131.
8. A. A. Al-Amiery, M. H. O. Ahmed, T. A. Abdullah, T. S. Gaazd and A. A. H. Kadhum, *Res. Phys.,* 9 (2018) 978.
9. C. Verma, J. Haque, E. E. Ebenso and M.A. Quraishi, *Res. Phys*., 9 (2018) 100.
10. J. Zhang, L. Zhang, G. Tao and N. Chen, *Int. J. Electrochem. Sci*., 13 (2018) 8645.
11. K. F. Al-Azawi, I. M. Mohammed, S. B. Al-Baghdadi, T. A. Salman, H. A. Issa, A. A. Al-Amiery, T. S. Gaaz and A. A. H. Kadhum, *Res. Phys*., 9 (2018) 278.
12. E. Marsault and M. L. Peterson, *J. Med. Chem*., 54 (2011) 1961.
13. H. S. Soor, S. D. Appavoo and A. K. Yudin, *Bioorgan. Med. Chem*., 26 (2018) 2774.
14. M. Shin, H. Ju, Y. Habata and S. S. Lee, *Inorg. Chim. Acta*, 482 (2018) 482 749.
15. V. V. Syakaeva, J. E. Morozova, A. V. Bogdanov, Y. V. Shalaeva, A. M.E rmakova, A. D. Voloshina, V. V. Zobov, I. R. Nizameev, M. K. Kadirov, V. F. Mironov and A. I. Konovalov, *Colloid. Surf. A: Physicochem. Engin. Aspe*., 553 (2018) 368.
16. S. Brooker, *Coordin. Chem. Rev.,* 222(2001) 33.
17. J. Costamagna, G. Ferraudi, B. Matsuhiro, M. C. Vallette, J. Canales, M. Villagrán, J. Vargas and M. J. Aguirre, *Coordin. Chem. Rev.,* 1996 (2000) 125.
18. W. Gou, C. Lai and Z. Xiang, *Int. J. Electrochem. Sci*., 12 (2017) 9983.
19. W. Gou, C. Lai, Z. Xiang, L. Yang, P. Zhang, W. K. Xie, L. Chen, G. B. Luo, X. L. Li and Z. X. Chen, *Int. J. Electrochem. Sci*., 12 (2017) 11742.
20. B. E. Douglas, *Inorganic Syntheses*, 18(1978) 1
21. J. Haque, C. Verma, V. Srivastava, M. A. Quraishi and E. E. Ebenso, *Res. Phys*., 9 (2018) 1481.
22. T. A. Salman, K. F. Al-Azawi, I. M. Mohammed, S. B. Al-Baghdad, A. A. Al-Amiery, T. S. Gaaz and A. A. H. Kadhum, *Res. Phys*., 10 (2018) 291.
23. S. Varvara, L. Găină, R. Bostan, F. Popa and A. Grozav, *Int. J. Electrochem. Sci.,* 13 (2018) 8338.
24. D. Fu, B. Tan, L. Lu, X. Qin, S. Chen, W. He and J. Chen, *Int. J. Electrochem. Sci.,* 13 (2018) 8561.

25. S. A. Umoren, A. A. AlAhmary, Z. M. Gasem and M. M. Solomon, *Int. J. Biol. Macromol*., 117 (2018)1017.
26. A. E. Somers, B. R. W. Hinton, C. B. Dickason, G. B. Deacon, P. C. Junk and M. Forsyth, *Corros. Sci.,* 139 (2018) 430.
27. M. A. El-Raouf, E. A. Khamis, M. T. H. A. Kana and N. A. Negm, *J. Mol. Liq*., 255 (2018) 341.
28. C. D. Wang, C. Lai, B. Xie, X. G. Guo, D. Fu, B. Lia nd S. S. Zhu, *Res. Phys*., 10 (2018) 558.